Anal Bioanal Chem (2009) 393:1151–1156
DOI 10.1007/s00216-008-2370-8

ORIGINAL PAPER

Prostate-specific antigen immunoassays on the BioCD

Xuefeng Wang · Ming Zhao · David D. Nolte

Received: 8 July 2008 / Revised: 20 August 2008 / Accepted: 22 August 2008 / Published online: 15 September 2008

Abstract The BioCD is a spinning-disc interferometric biosensor on which antibodies are immobilized to capture target antigens from biological samples. In this work, BioCDs measured the interferometric response to prostate-specific antigen (PSA). The ideal detection limit for PSA was determined using a BioCD with 12,500 printed target antibody spots with a corresponding number of reference protein spots. Statistical analysis projects the detection limit of PSA as a function of the number of spots included in the average. When approximately 10,000 spot pairs were averaged, the 3σ detection limit was 60 pg/ml in a 2 mg/ml simple protein background. A standard format for BioCD immunoassays uses 96 wells with 32 target spots paired with reference spots. In serum, the detection limit for this format was 1 ng/ml in 3:1 diluted female human serum using a sandwich assay with a nonfluorescent mass tag.

Keywords Optical biosensor · BioCD · Label-free · Prostate cancer · Prostate-specific antigen · Antibody microarray

Introduction

Many diseases cause protein-level variations in human body fluids. The corresponding protein concentrations can act as the diagnostic markers for these diseases. Simultaneous measurement of hundreds of protein concentrations would provide valuable information for diagnosis and prognosis. For instance, p73 and $p57^{Kip2}$ are believed to be prognostic markers for acute lymphocytic leukemia [1], and prostate-specific antigen (PSA) is the marker for prostate cancer, which accounts for 10% of all deaths from cancer [2]. This paper focuses on the detection of PSA. PSA is a member of the kallikrein family exclusively produced by the prostate gland. It has a concentration of 0.5–2.0 mg/ml in normal seminal fluid [3, 4] and 0–4 ng/ml in serum [5]. Prostate cancer and other prostate pathological changes may cause PSA to leak into the peripheral circulation [6, 7] and induce an abnormal elevation of the PSA level in serum. Levels higher than 10 ng/ml may suggest the presence of prostate cancer; however, prostate cancer can be present without PSA level elevation [8], while PSA levels may increase owing to other prostate disorders or diseases [9, 10]. Because of the high rate of false negatives and false positives, a PSA test alone cannot give a confident diagnosis for prostate cancer. Research on the ratio of free PSA and bound PSA [11] suggests that the pattern of multiple protein levels may have a better chance to uniquely identify certain diseases. Undoubtedly, the measurement of the protein "fingerprint" demands a large-scale and high-throughput immunoassay method.

In this paper, we lay the groundwork for the BioCD as a feasible platform to realize simultaneous large-scale immunoassays. The high-level multiplexing would be made possible through interferometric detection. To perform the interferometric detection of an antigen, we immobilize an antibody monolayer (around 1–1.5-nm thickness) in a spot pattern on a dielectric surface with a reflection coefficient engineered to convert optical phase to optical intensity. The

X. Wang (✉) · M. Zhao · D. D. Nolte
Department of Physics, Purdue University,
525 Northwestern Avenue,
West Lafayette, IN 47907-2036, USA
e-mail: wang137@purdue.edu

area mass density of protein is detected by monitoring the reflection change due to the protein layer. Compared with traditional antibody microarrays, which require fluorophores or other chemical labels to detect the presence of protein, the BioCD has the advantage of performing quantitative measurements with no need for a fluorescent label (but augmented by mass labels in a sandwich configuration). We adopted a common-path design [12] and spinning-disc interferometry to construct the BioCD scanning system. The common-path configuration makes the signal stable, and spinning the disc suppresses the noise floor by 40 dB [13]. While other nonfluorescent techniques have been developed, such as surface plasmon resonance [14–16] and ellipsometry [17–19], that also have the advantage of requiring no fluorescent labels, these approaches rely on detailed surface structuring or fabrication under tight constraints or high incidence angles. The BioCD, in contrast, has a simple structure and operation that makes it robust and easy to manufacture. A comparison between these methods and the BioCD is given in [20, 21].

In our preliminary exploration on the application of the BioCD for multiplexed PSA detection, we fabricated anti-PSA BioCDs in two formats: 96-well and 25,000-spot using sandwich assays. The 96-well format was implemented to find the concentration response of the PSA assay on the BioCD. The 25,000-spot format was designed to explore the limit of detection for PSA as a function of the number of target-reference spot pairs. Although the sandwich assay is not label-free, it is used to measure the concentration of PSA in a high protein background by distinguishing specific binding from nonspecific binding.

Materials and methods

This section describes the operational principles of interferometric detection on the BioCD, including the laser scanning system and the spot-based formats of the discs.

BioCD theory and structure

The BioCD is a platform that accommodates thousands of printed antibody spots using an optical detection technique that detects the bound analyte directly with interferometry. A layer of antibody molecules is immobilized on a thermal oxide on a silicon wafer that has a diameter of 100 mm. The surface of the wafer is aldehyde-functionalized and able to covalently bind with protein. The protein layer alters the reflection coefficient of the BioCD surface, and the protein-induced change is optimized by selecting the proper thickness of the SiO_2 layer. By monitoring the reflection change due to immunobinding, one can measure the quantity of bound antigen.

Given a surface with reflection coefficient r, the reflection is changed into r' after applying a thin (much less than the probe wavelength) protein layer [20],

$$r' = r + \left[\frac{(r_p - r)(1 - rr_p)}{\left(1 - r_p^2\right)} + r\frac{\tan\theta_p}{\tan\theta_0}\right] \times \frac{4i\pi d n_p \cos\theta_p}{\lambda}, \quad (1)$$

where λ is the probe wavelength, θ_0 is the incidence angle, n_p and d are the refractive index and the thickness of the protein layer, $n_p\sin\theta_p = \sin\theta_0$, and r_p is the reflection coefficient of the air-to-protein interface.

Under the condition of s-polarization, the reflection coefficient is $r_p = \frac{\sin(\theta_p - \theta_0)}{\sin(\theta_p + \theta_0)}$ and equation 1 is further simplified to

$$r' = r + \frac{(1+r)^2}{\cos\theta_0}\frac{\pi i}{\lambda}\left(1 - n_p^2\right)d, \quad (2)$$

Using the laser scanning system (described later), we scan the entire disc to acquire a 2D image of the protein profile by detecting the reflectance variation r' caused by the protein layer. With the assumption $d << \lambda$, the signal is approximately

$$S(x,y) = |r'(x,y)|^2 - |r|^2 = Im\left[(1+r)^2\bar{r}\right]\frac{2\pi}{\lambda\cos\theta_0} \times \left(n_p^2 - 1\right)g^2(x,y) \otimes d(x,y), \quad (3)$$

where $d(x, y)$ is the protein layer topology on the wafer, $g(x, y)$ is the Gaussian beam profile, and $\bar{r}$ is the complex conjugate of r.

From equation 3, the intensity of the signal is determined by the protein layer thickness, the refractive index of the protein, the incident angle, the probe wavelength, and the term $\mathrm{Im}\left[(1+r)^2\bar{r}\right]$. $\mathrm{Im}\left[(1+r)^2\bar{r}\right]$ is the protein-to-intensity conversion factor, which can be selected for an optimized r that maximizes the conversion at extrema of ∓ 0.385 at $r = \pm 0.577i$ ($|r|$ is always less than 1).

Our current BioCD structures use a silicon wafer with a 120-nm SiO_2 thermal oxide layer. At a wavelength of 488 nm with s-polarization and 30° incidence, the wafer reflection coefficient is $r = -0.049 + 0.489i$, giving a conversion factor of 0.371, which is close to the optimum value of 0.385. A 1-nm protein layer induces 0.0056 absolute reflectance change, or 2.2% ratio increment. Therefore, the 120-nm SiO_2 layer on silicon is highly sensitive and simple to implement.

BioCD scanning system

The experimental layout of the disc and laser system is shown in Fig. 1. The probe light is incident at 30° on the

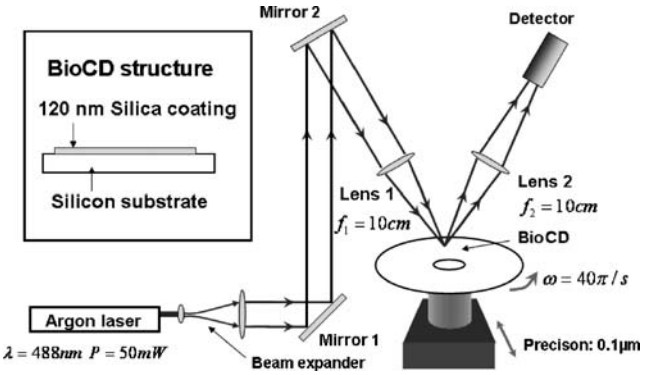

Fig. 1 Optical layout for the laser disc scanning. The BioCD is mounted on a motor on a linear stage. A computer controls the motion of the motor and the stage to generate 2D scanning with polar coordinates. A 488 nm argon laser provides the probe light. The light is focused on the BioCD and reflected into a silicon detector. The reflectance variation due to protein is detected and sent to the computer via an oscilloscope

disc with s-polarization. The polarization condition is not essential, and p-polarization is equally possible. This direct interferometric approach also works at normal incidence, but we chose the oblique incidence for convenience. The laser is an INNOVA 300 argon laser (Coherent) using a wavelength of 488 nm. A 10 cm focal length convex lens is used to focus the laser beam onto the disc surface. The radius of the focal spot is 18 μm on the disc. Higher resolution can be achieved by switching the 10 cm focal length lens for a short focal length lens. Reflected light is guided into a detector which acquires the signal. The detector responsivity is 0.2 A/W with a dark noise level of 8.3 μW.

The BioCD is positioned on a motor (Lincoln Laser) which spins with a selectable frequency between 20 and 80 Hz. The motor is fixed on a linear translation stage (MM2000, Newport) that moves back and forth with 0.1-μm linear precision and 300-mm maximum travel distance. The motor and the linear stage form a polar coordinate system to acquire a 2D map of the disc with appropriate computer control. In the experiments reported here, we used a rotation frequency of 20 Hz and a 15-μm linear step (radius pitch). The protein topology is detected by calculating the relative intensity signals and reconstructing them into a 2D image.

Sandwich assay and BioCD formats

Because the PSA molecule has a relatively small molecular mass, about 28 kDa [22], the forward-phase assay has a weak response; therefore, we adopted a nonfluorescent sandwich assay to boost the detection sensitivity. We immobilized the antibody on the BioCD in a printed spot pattern consisting of pairs of target antibody spots and reference protein spots [usually immunoglobulin G (IgG) molecules], and then incubated the antibody spots in an analyte-containing solution. The target protein is captured by the antibody spots and is therefore also immobilized on the BioCD. A scan after incubation with the analyte was performed to record the protein profile across the entire disc. After the postincubation scan, the protein spots were exposed to a solution containing a secondary antibody. The post-secondary-antibody scan was performed to record the new protein profile. The protein spot height increments were calculated by subtracting the postincubation scan data from the post-secondary-antibody scan data. Height increments yield the amount of bound secondary antibody, which is related to the target protein concentration in the incubated sample solution.

Two types of BioCD formats were used for this work. A 96-well BioCD was designed to explore the response curve for target protein using a concentration ladder spanning several orders of magnitude. In the 96-well configuration, 6-mm-diameter rings are printed with ultrahydrophobic ink on the disc. These rings create 96 subregions surrounded by the hydrophobic boundary to perform separate assays on a single disc (Fig. 2 shows the incubation with different concentrations in 96 wells). The second type of BioCD spot format used 25,000 spots and was designed to explore detection limits of target protein concentration. This disc had no hydrophobic boundaries, and the entire disc was exposed to a single analyte concentration.

PSA assay on a 96-well anti-PSA BioCD

The 96-well BioCD was used to establish the response curve of the PSA immunoassay. The 120-nm thermal oxide of the silicon disc surface was aldehyde-functionalized to bind protein covalently. Butyraldehyde was grafted on the SiO_2 surface to cause the carbonyl group of butyraldehyde to react with the amino groups of the antibody to form a Schiff base which immobilizes the antibody molecules. A Scienion (BioDot) piezoelectric printer was used to print 32 antibody spots (anti-PSA produced in goat, G-126-C, Biospacific) and 32 reference spots (antirabbit IgG produced in goat, R2004, Sigma) in each of 96 wells (Fig. 2). The diameter of each spot was approximately 150 μm, with a spot-to-spot separation of approximately 300 μm. After printing, the land of the disc was blocked by casein solution [phosphate-buffered saline (PBS) +1% casein solution in 20:1 volume ratio, pH 8.0], washed by 50 mM citric acid solution (pH 6.0), PBS +0.05% Tween (PBST), and deionized water, and spun dry at 300 rpm.

After printing, 90 wells were incubated with PSA (30-AP16, Fitzgerald) solution ranging in concentration from 0 to 3,000 ng/ml in PBST and either 20:1 or 3:1 diluted female human serum for 1 h. A postincubation scan was performed to record the original protein profile across the entire disc. Figure 2 shows two typical wells with post-

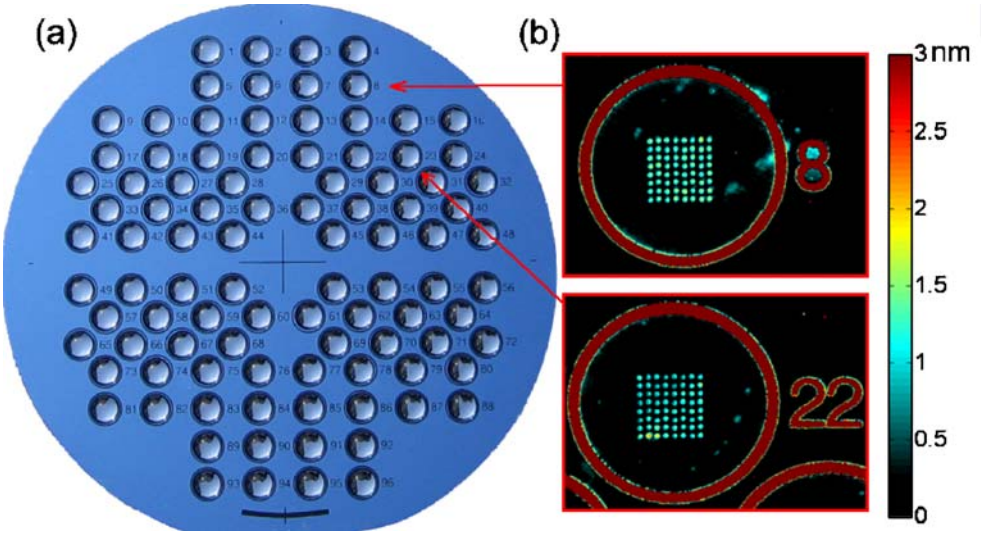

Fig. 2 **a** Overview of the 96-well anti-prostate specific antigen (PSA) BioCD. The 96 wells are used for multiplexed assays. The picture shows simultaneous incubation at different concentrations in 96 wells. Ultrahydrophobic boundaries confine the solutions in the wells. **b** Two typical wells are shown at the postincubation scan. Each well contains 32 anti-PSA spots and 32 reference spots with diameters of 150 μm. Each anti-PSA spot is adjacent to a reference spot. The thickness of each spot is around 1–1.5 nm

incubation protein signals. For the sandwich assay, all wells were incubated with 20 μg/ml anti-PSA, and then a postsandwich scan was performed. The immunobinding due to captured PSA binding secondary antibody was found by subtracting the postincubation scan data from the postsandwich scan data.

PSA assay on 25,000-spot anti-PSA BioCD

This nonsegmented disc was used to establish the detection limit of PSA with a large number of antibody spots. In this case, the disc had no hydrophobic boundaries. Instead, 12,500 antibody spots (anti-PSA produced in goat, G-126-C, Biospacific) and 12,500 reference spots (antirabbit IgG produced in goat, R2004, Sigma) were printed across the entire disc. Each antibody spot was paired with a reference spot. The diameter of each spot was approximately 150 μm (Fig. 3). We detected the response on the 25,000 spots to a 10 ng/ml concentration of PSA and estimated the scaling detection limit by statistical extrapolation.

The sample solution was created by spiking PSA (30-AP16, Fitzgerald) into bovine serum albumin solution. The final concentration was 10 ng/ml for PSA in 2 mg/ml background bovine serum albumin. The buffer was a PBS solution with 0.05% Tween (PBST) to suppress nonspecific binding. The anti-PSA BioCD was incubated with the sample solution on an orbital shaker for 3 h to allow the antigen and the antibody to reach binding equilibrium. The BioCD was rinsed with deionized water and dried using a pure nitrogen stream. A postincubation scan was performed to record the initial protein profile across the entire disc, and the thicknesses of each spot were calculated.

The BioCD was then incubated with 10 μg/ml goat anti-PSA antibody (G-126-C, Biospacific). The second antibody had no fluorescent tag. The BioCD was rinsed with deionized water and dried with dry nitrogen. The post-

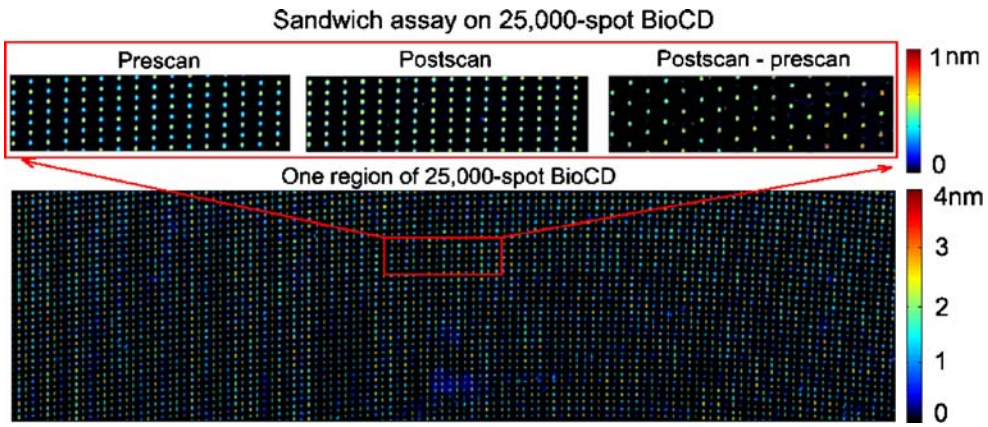

Fig. 3 Overview of the 25,000-spot anti-PSA BioCD: 12,500 anti-PSA and 12,500 reference spots are printed in pairs on an entire disc. Examples of prescan (postincubation against 10 ng/ml PSA concentration), postscan (postsandwich), and the difference between two scans are shown in the upper sections. Anti-PSA spots have a significant thickness increment (about 0.5 nm) compared with the reference spots. The specific increment is due to the immunobinding between the PSA and the secondary anti-PSA molecules (in the sandwich assay)

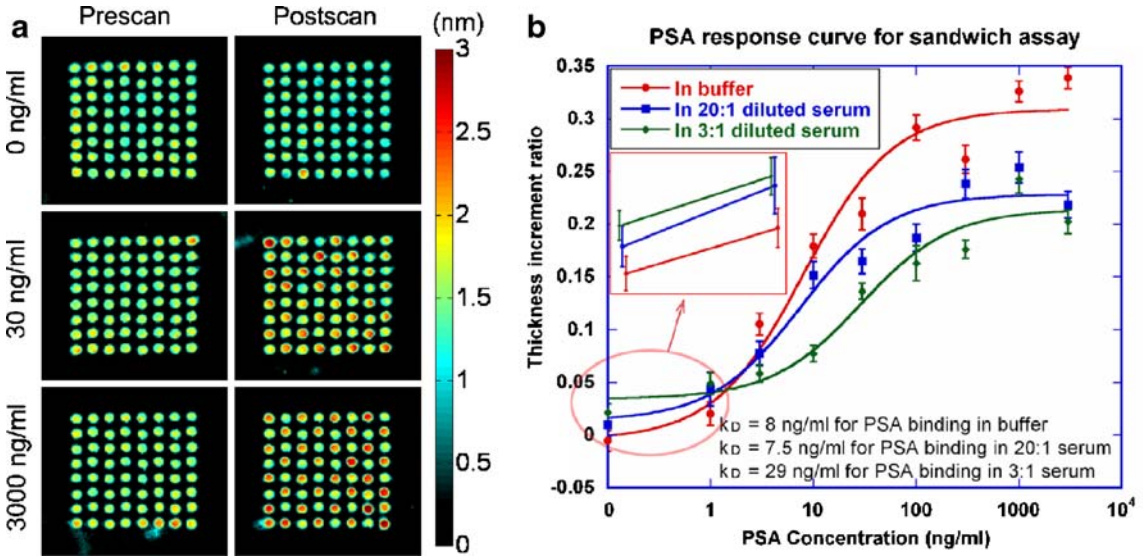

Fig. 4 **a** Assay responses at different concentrations. Three typical wells (well 3 at 0 ng/ml assay, well 24 at 30 ng/ml, and well 1 at 3 μg/ml) are shown for the prescan and the postscan. **b** Response curves for PSA sandwich assays in buffer, in 20:1 diluted serum, and in 3:1 diluted serum (concentrations of PSA 0, 1, 3, 10, 30, 100, 300, 1,000, 3,000 ng/ml). The assay at 1 ng/ml has a stronger response than that at 0 ng/ml, and the detection limit is around 1 ng/ml with 160 anti-PSA spots according to 3σ criteria for detection limit evaluation. (Each concentration assay consists of five wells, with 160 pairs of target and reference spots.)

sandwich scan was performed to obtain the new thicknesses of each spot. By registering the postincubation scan and the postsandwich scan data and subtracting the thicknesses for each spot (Fig. 3), we calculated the immunoassay response and estimated the detection limit.

Results and discussion

PSA response curve

The results of the 96-well nonfluorescent sandwich assay are shown in Fig. 4. The response curves show monotonic increasing dependence on the antigen concentration applied during the incubation. The curves are fitted with the Langmuir equation, and the equilibrium constants for the immunobinding reaction are approximately K_D=8 ng/ml in the 20:1 diluted serum and in the buffer, and K_D=29 ng/ml in the 3:1 diluted serum. The higher value might be induced by competition with the background protein. By comparing the assay at 0 ng/ml with that at 1 ng/ml, we found positive responses in both sera and buffer, and according to 3σ criteria (the assay response at detection-limit concentration equals 3 times the standard deviation of the responses for blank samples), the detection limit is around 1 ng/ml in 3:1 human serum using a population of 160 target antibody

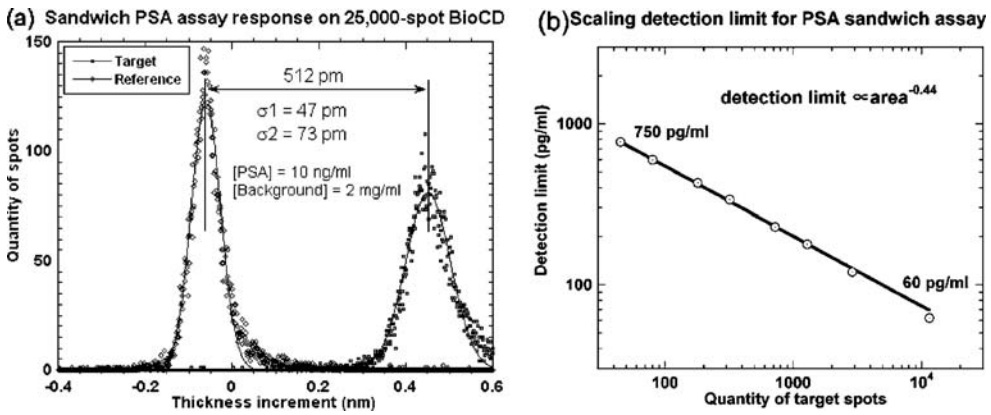

Fig. 5 **a** Histogram of thickness increments of 25,000 spots incubated at 10 ng/ml after secondary antibody incubation. On the basis of the mean values and standard deviations of the distributions, the detection limit of one pair of antibody and reference spots is estimated to be 5 ng/ml in 2 mg/ml background concentration. **b** The scaling PSA detection limits of the sandwich assay are shown. The scaling detection limit is fit by a power law with exponent −0.44 instead of −0.5. A 60 pg/ml detection limit for the PSA sandwich assay is achieved based on 11,520 antibody spots, and it is 750 pg/ml based on 45 spots

spots distributed across five wells. The normal PSA level in serum is around 4 ng/ml, and pathological change of the prostate gland causes elevation of PSA levels; the 96-well anti-PSA BioCD is sensitive enough to measure abnormal PSA levels.

PSA detection limit as a function of spot averaging

The thickness increments for all spots are shown as histograms in Fig. 5a and fitted with normal distributions for both the target and the reference spots. The mean value and the standard deviation of the immunological responses are-62 and 47 pm for reference spots and 450 and 73 pm for anti-PSA spots. The height distributions of the antibody and reference spots are well distinguished from each other. With 10 ng/ml PSA concentration in the sample solution, according to 3σ criteria, the detection limit of one pair of antibody and reference spots is estimated to be $10 \times 3 \times \sqrt{0.073^2 + 0.047^2}/(0.512) = 5(\mathrm{ng/ml})$.

With larger populations, the detection limit can be improved because the standard error is inversely proportional to the square root of the population size (number of antibody spots); however, the intrawell and interwell spot height variations also limit the detection limit. More spots require a larger printing area, and a larger area produces larger surface variations. These types of spatial correlation modify the square-root scaling. To verify the power law and find the correct exponent, we divided up all spots into local subpopulations. There were m subpopulations each with n antibody spots constrained by the product $m \times n \approx 12{,}500$. The detection limit of each subpopulation was calculated using the standard error, then averaged over the m subpopulations. The average was treated as the scaling detection limit for a population with n spots. The relation between the scaling detection limit and the population size is shown in Fig. 5b. The scaling detection limit is proportional to the number of spots fit to a power law with exponent −0.44 instead of −0.5. The 3σ detection limit varies from 60 pg/ml based on a population of 11,520 antibody spots (the other 980 spots are discarded for relatively poor printing quality) to 750 pg/ml based on 45 anti-PSA spots.

Conclusion

We performed PSA sandwich assays on BioCDs in two formats: 96-well BioCDs and 25,000-spot BioCDs. From the results of the 96-well assays, we acquired the response curve of PSA and found an equilibrium binding constant of 8 ng/ml for binding of PSA and anti-PSA. The detection limit for PSA was below 1 ng/ml in buffer and 20:1 and 3:1 diluted female serum, and the BioCD sensitivity for PSA detection reaches the clinical level (4 ng/ml in the undiluted serum). The assays on the 25,000-spot BioCDs showed a 60 pg/ml detection limit based on a population of 11,520 antibody spots. The scaling detection limit based on different numbers of spots was found to have a power-law relation with the number of spots with an exponent of −0.44 instead of −0.5. The 96-well and the 25,000-spot BioCDs provided two different assay modes for two different purposes. The 96-well BioCD is suitable for simultaneous multiple assays on a single disc, while the 25,000-spot BioCD is used to determine the scaling detection limits.

Acknowledgements This work was sponsored under grants from Quadraspec Inc. and from the Indiana Economic Development Corporation through the Purdue Research Foundation. We thank Sven Schreiber, Benjamin Edquist, and other staff at Quadraspec Inc. for help in printing the antibody microarray and advice on BioCD surface chemistry.

References

1. Bueso-Ramos C, Xu YL, McDonnell TJ, Brisbay S, Pierce S, Kantarjian H, Rosner G, Garcia-Manero G (2005) J Clin Oncol 23:3932–3939
2. Ozen H, Sozen S (2006) Eur Urol Suppl 5:495–499
3. Wang MC, Papsidore LD, Kuriyama M, Valenzuela LA, Murphy GP, Chu TM (1981) Prostate 2:89–96
4. Lovgren J, Valtonen-Andre C, Marsal K, Lilja H, Lundwall A (1999) J Androl 20:348–355
5. Catalona WJ, Richie JP, Ahmann FR, Hudson MA, Scardino PT, Flanigan RC, Dekernion JB, Ratliff TL, Kavoussi LR, Dalkin BL, Waters WB, Macfarlane MT, Southwick PC (1994) J Urololgy 151:1283–1290
6. Brawer MK, Rennels MA, Nagle RB, Schifman R, Gaines JA (1989) Am J Clin Pathol 92:760–764
7. Bostwick DG (1994) Am J Clin Pathol 102:S31–S37
8. Thompson IM, Pauler DK, Goodman PJ, Tangen CM, Lucia MS, Parnes HL, Minasian LM, Ford LG, Lippman SM, Crawford ED, Crowley JJ, Coltman CA (2004) New Engl J Med 350:2239–2246
9. Herschman JD, Smith DS, Catalona WJ (1997) Urology 50:239–243
10. Crawford ED, Schutz MJ, Clejan S, Drago J, Resnick MI, Chodak GW, Gomella LG, Austenfeld M, Stone NN, Miles BJ, Thomson R (1992) JAMA 267:2227–2228
11. Catalona WJ, Partin AW, Slawin KM, Brawer MK, Flanigan RC, Patel A, Richie JP, deKernion JB, Walsh PC, Scardino PT, Lange PH, Subong ENP, Parson RE, Gasior GH, Loveland KG, Southwick PC (1998) JAMA 279:1542–1547
12. Dyson J (1957) J Opt Soc Am 47:386–390
13. Zhao M, Wang X, Nolte D (2007) Proc SPIE 6447:64470B
14. Johnson B, Löfas S, Lindquist G (1991) Anal Chem 198:268–277
15. Jonsson U, Fagerstam L, Ivarsson B, Johnsson B, Karlssson R, Lundh K, Lofas S, Persson B, Roos H, Ronnberg I, Sjolander S, Stenberg E, Stahlberg R, Urbaniczky C, Ostilin H, Malmqvist M (1991) BioTechniques 11:620–627
16. Homola J, Yee S, Gauglitz G (1999) Sens Actuators B Chem 54:3–15
17. Malmsten M (1994) J Colloid Interface Sci 166:333–342
18. Landgren M, Jonsson B (1993) J Phys Chem 97:1656–1660
19. Lousinian S, Logothetidis S (2007) Microelectron Eng 84:479–485
20. Wang X, Zhao M, Nolte D (2007) Appl Opt 46:7836–7849
21. Gauglitz G (2005) Anal Bioanal Chem 381:141–155
22. Belanger A, Vanhalbeek H, Graves HCB, Grandbois K, Stamey TA, Huang LH, Poppe I, Labrie F (1995) Prostate 27:187–197